



Crustal resistivity structure of the southwestern transect of the Rif Cordillera (Morocco)

Farida Anahnah, Jesus Galindo-Zaldivar, Ahmed Chalouan, Jaume Pous, Patricia Ruano, Antonio Pedrera, Ana Ruiz-Constan, M'Fedal Ahmamou, Mohamed Benmakhlouf, Pedro Ibarra, et al.

► To cite this version:

Farida Anahnah, Jesus Galindo-Zaldivar, Ahmed Chalouan, Jaume Pous, Patricia Ruano, et al.. Crustal resistivity structure of the southwestern transect of the Rif Cordillera (Morocco). *Geochemistry, Geophysics, Geosystems*, 2011, 12, pp.Q12016. <10.1029/2011GC003783>. <hal-00670999>

HAL Id: hal-00670999

<https://hal.science/hal-00670999v1>

Submitted on 27 Sep 2021

HAL is a multi-disciplinary open access archive for the deposit and dissemination of scientific research documents, whether they are published or not. The documents may come from teaching and research institutions in France or abroad, or from public or private research centers.

L'archive ouverte pluridisciplinaire **HAL**, est destinée au dépôt et à la diffusion de documents scientifiques de niveau recherche, publiés ou non, émanant des établissements d'enseignement et de recherche français ou étrangers, des laboratoires publics ou privés.



Copyright - All rights reserved



Crustal resistivity structure of the southwestern transect of the Rif Cordillera (Morocco)

Farida Anahnah

Departamento de Geodinámica, Universidad de Granada, E-18071 Granada, Spain

Jesús Galindo-Zaldívar

Departamento de Geodinámica, Universidad de Granada, E-18071 Granada, Spain (jgalindo@ugr.es)

Also at IACT, CSIC, Universidad de Granada, E-18071 Granada, Spain

Ahmed Chalouan

Département de Géologie, Université Mohammed V-Agdal, 10106 Rabat, Morocco

Jaume Pous

Departament de Geodinàmica i Geofísica, Universitat de Barcelona, E-08028 Barcelona, Spain

Patricia Ruano

Departamento de Geodinámica, Universidad de Granada, E-18071 Granada, Spain

Also at IACT, CSIC, Universidad de Granada, E-18071 Granada, Spain

Antonio Pedrera

Instituto Geológico y Minero de España, E-18071 Granada, Spain

Ana Ruiz-Constán

Géosciences, Université Montpellier 2, Sciences et Techniques, F-34095 Montpellier CEDEX 05, France

M'Fedal Ahmamou

Département de Géologie, Université Mohammed V-Agdal, 10106 Rabat, Morocco

Mohamed Benmakhlouf

Département de Géologie, Université Abdelmalek Essaadi, 93003 Tetuán, Morocco

Pedro Ibarra

Instituto Geológico y Minero de España, E-18071 Granada, Spain

Eva Asensio

Departament de Geodinàmica i Geofísica, Universitat de Barcelona, E-08028 Barcelona, Spain

[1] A NE-SW magnetotelluric 110 km-long profile including 18 sites was acquired across the western Rif Cordillera along the Eurasian-African plate boundary, allowing to constrain its poorly known deep structure. It extends from the Internal Zones, close to the Alboran coast, crossing the External Zones and up to the Gharb foreland basin. The periods recorded range from 0.001 s to 1000 s. The combination of magnetotelluric data with available geological data provides new insight regarding the relationship

between deep and shallow crustal structures of the Rif Cordillera. Analyses of structural dimensionality suggest a preferential NW-SE direction, and a 2D joint inversion was performed. A 3D inversion extending the 2D model along the strike confirmed the reliability of this approach. The magnetotelluric model shows a heterogeneous upper crust in agreement with the geological structures observed at surface. The Internal Zones correspond to resistive (metamorphic rocks) and conductive (peridotites) bodies, while the External Zones and the foreland basin are characterized by large conductive bodies of variable thickness. A crustal detachment level separating shallow geological units from a probable variscan basement was inferred. At depth, the most relevant feature consists of large resistive bodies with a shallow irregular top, located below the frontal part of the Rif. The outcrops of exotic metapelitic, granitic and gneissic blocks in the frontal part of the Cordillera suggest that these large resistive bodies may correspond to a gneissic or granitic basement surrounded by metapelitic rocks. Late contractive thrust and diapiric processes were responsible for their uplift and shallow emplacement. The Rif constitutes an active southwestward vergent orogenic wedge, oblique to the present-day NW-SE convergent Eurasian-African plate boundary.

Components: 6700 words, 10 figures.

Keywords: Gibraltar Arc; broadband magnetotelluric; crustal detachments; deep structure; exotic blocks.

Index Terms: 0925 Exploration Geophysics: Magnetic and electrical methods (5109); 8038 Structural Geology: Regional crustal structure; 8110 Tectonophysics: Continental tectonics: general (0905).

Received 8 July 2011; **Revised** 19 October 2011; **Accepted** 24 October 2011; **Published** 21 December 2011.

Anahnah, F., et al. (2011), Crustal resistivity structure of the southwestern transect of the Rif Cordillera (Morocco), *Geochem. Geophys. Geosyst.*, 12, Q12016, doi:10.1029/2011GC003783.

1. Introduction

[2] The Gibraltar Arc, formed by the alpine Betic and Rif Cordillera, surrounds the western Alboran Sea (Figure 1) and is located on the NW-SE convergent Eurasian-African plate boundary. In this region of widespread deformation, arched geometry is one consequence of the complex interaction of the westward migration of the Alboran domain in between the Eurasian and African plates. Several tectonic models have been proposed up to present, involving one or several subduction zones with or without roll-back [Morley, 1993; Royden, 1993; Lonergan and White, 1997; Fadil et al., 2006; Brun and Faccenna, 2008], delamination [Platt and Vissers, 1989; Seber et al., 1996; Calvert et al., 2000] and other hypotheses such as mantle diapirism [Weijermars et al., 1993]. Although most of them try to account for available geophysical and geological data, they lack detailed geophysical constraints on the deep structure. In this setting, the Rif cordillera deep continental crust is quite poorly known, despite detailed reports of surface geology. The presence of thrusts and low angle normal faults produces a decoupling at different crustal levels. Moreover, the scarce geophysical data (gravity [Van den Bosch, 1971, 1981; Bellot, 1985] and seismic

refraction [Hatzfeld and Ben Sari, 1977]) points to great heterogeneities in the crust and the mantle while only providing regional insights as to the deep structure.

[3] The aim of this study is to present the first magnetotelluric profile of the southwestern transect of the Rif Cordillera and Gharb basin and analyze their crustal structural features. 2D and 3D inversions of these data were carried out. The resistivity model was integrated with geological data (Figure 1) to constrain the relationships between shallow and deep crustal structures and discuss the features of the main discontinuities. Moreover, we provide new data to discuss the origin of exotic granites, gneiss, and metapelitic blocks that outcrop in the frontal Rif cordillera.

2. Geological Setting

[4] The study area belongs to the westernmost end of the Mediterranean Alpine belt. The Rif cordillera (Figure 1), situated in northern Morocco, formed together with the Betic cordillera as a consequence of the westward motion of the Alboran Domain between northwest Africa and Iberia since the early Tertiary. In addition, this process is interacting with the N-S to NW-SE convergence between Africa

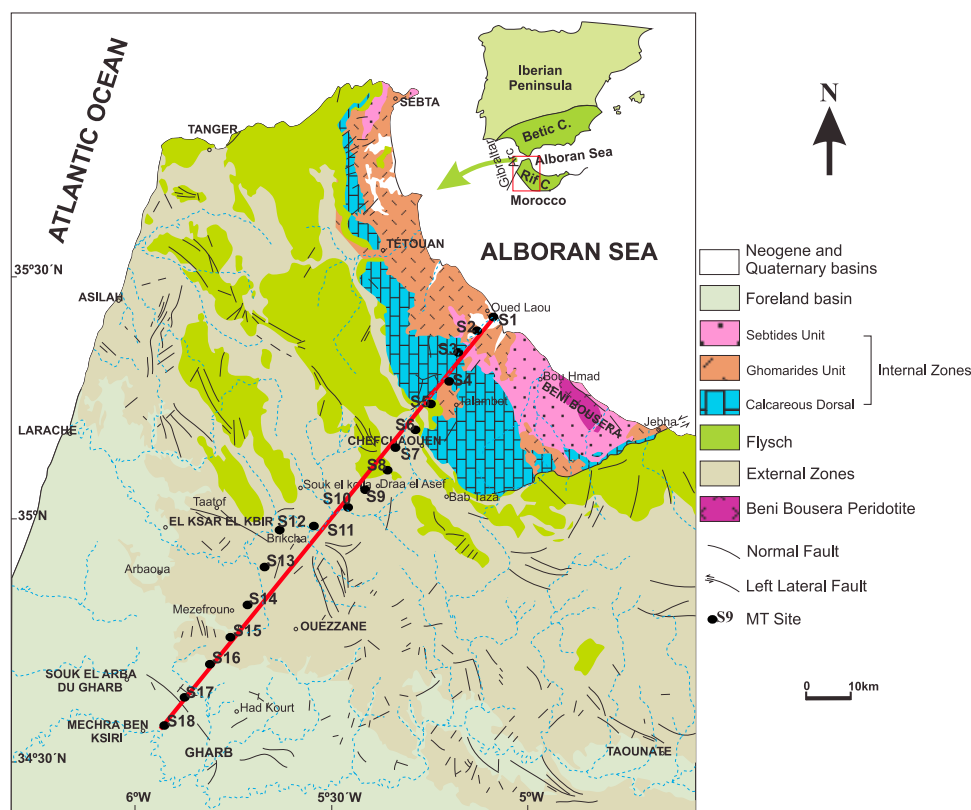


Figure 1. Geological map of the western Rif Cordillera showing the location of the MT profile.

and Eurasia. We focus this contribution on the southwestern Rif transect (Figure 1).

[5] The Rif cordillera (Figure 1) includes the Internal and the External Zones, separated by Flysch units, as in other alpine Mediterranean cordilleras. The tectonic structure orientations are comprised between ENE-WSW in the Eastern Rif, to NNW-SSE at the tip of the Western Rif.

[6] The Internal Zones of the study area are formed by Palaeozoic, Mesozoic and Cenozoic sequences, including three main metamorphic complexes affected by alpine deformation and partially by metamorphism since the Eocene-Late Oligocene. They are: the Sebide, the Ghomaride and the Dorsal complexes. They thrust to the SW on the Flysch units and External Zones and are bounded to the SE by the Jebha fault (Figure 1), a major transfer fault produced during the westward emplacement of the Rif units. The Sebide complex is a stack of metamorphic units [Kornprobst, 1974; Michard et al., 1983; Saddiqi, 1995; Bouybaouene et al., 1998]. It includes the Beni Bousera peridotites, overlain by granulites, gneisses, schists, Permian-Triassic phyllites and quartzites, and Triassic carbonates of the upper units. The Ghomaride complex includes four nappes of low-grade

Paleozoic metasediments covered by thick, unconformable Triassic red beds, and much thinner Liassic, Paleocene-Eocene limestones and Oligo-Miocene post-nappe detrital deposits [Chalouan and Michard, 1990; Maaté, 1996]. The Dorsal complex consists of stacked Late Triassic-Liassic carbonate sheets, with a thin cover of Jurassic-Late Cretaceous pelagic and Tertiary detrital sediments [Nold et al., 1981; El Kadiri et al., 1992]. The Sebide and Ghomaride units constitute the basement of the Alboran Sea, which is the largest Neogene basin in the region.

[7] The Flysch units are composed of Cretaceous-Lower Miocene detritic rocks. They generally overthrust the External Zones with the exception of some klippe that are located on the Internal Zones as the result of a complex evolution involving backthrusting or backsliding [Lepinasse, 1975; Chalouan et al., 1995; El Mirihi, 2005]. The External Zones are formed by units with generally carbonate and pelitic mesozoic and cenozoic series, mainly including limestones and marls. They are also locally affected by alpine low-grade metamorphism [Frizon de Lamotte, 1985; Azdimousa et al., 1998]. The External Rif consists of a fold- and thrust belt detached along the Late Triassic

evaporitic beds from the thinned continental crust of the North African margin [Suter, 1980; Wildi, 1983; Ben Yaich, 1991].

[9] The Gharb is a foreland subsiding basin located in the southwestern front of the Rif belt [Le Coz, 1964; Flinch, 1993; Zizi, 1996; Litto *et al.*, 2001]. This basin contains part of the Prérif Nappe surmounted by a large amount of continental sediments. It was moreover filled with sediments of marine origin (marls and sands) during the Tertiary and continental formations during the Quaternary, except for a coastal fringe [Cirac, 1987].

[10] After the main episodes of crustal thickening and metamorphism, in the Early Middle Miocene the region began to undergo E-W to NE-SW extension that led to the development of the Alboran Basin, floored by a thinned continental crust. Low- and high-angle normal faults [Benmakhlouf and Chalouan, 1995; Chalouan *et al.*, 1995; Saji and Chalouan, 1995] developed in the upper crustal levels.

[11] Recent compressional structures related to Eurasian-African convergence developing since the Late Miocene produce the main reliefs of the Rif Cordillera and increase the crustal thickness. The related structures are mainly large folds, reverse faults in the mountain front, and normal faults in the upper crustal levels of the Internal Zones. In addition, large strike-slip faults determine recent deformation in the Rif and allow for the escape of Central Rif toward the SW [Chalouan *et al.*, 2006].

[12] GPS data constrain the present-day tectonic motions, showing a top-to-the-SW displacement of the tectonic units in the Rif [Pérouse *et al.*, 2010; Vernant *et al.*, 2010]. The proposed model suggests that these displacements are related to crustal subduction toward the NE that occurs below the central part of the Rif and is associated with the intermediate seismicity of the Alboran Sea.

3. Previous Geophysical Data

[13] Seismic refraction [Hatzfeld and Ben Sari, 1977] studies reveal a 30 km thick continental crust, with a 9–10 km thick lower crust. Models that integrate both elevation and geoid gravity anomalies assuming local isostasy [Zeyen *et al.*, 2005] suggest a poorly marked orogenic root beneath the Central Rif cordillera that does not exceed 30 km. To the northeast, the Moho rises abruptly up to 18–20 km below the thin continental crust of the Alboran Basin.

[14] Seismic studies led Calvert *et al.* [2000] to suggest uprisen asthenosphere in the Alboran sea, floored by thinned continental crust, and even penetrating as a wedge between the Gibraltar Arc crust and underlying lithospheric mantle (in a delamination scenario). The model put forth by Fulla *et al.* [2007] points to somewhat greater thicknesses beneath the western Alboran sub-basin. Waveforms of body waves that traverse the Alboran Sea confirm the presence of an anomalous mantle underlying the basin [Bokermann and Maufroy, 2007].

[15] The 1:500,000 Bouguer gravity map of the Alboran Sea and Rif cordillera (Rabat sheets [Van den Bosch, 1971, 1981]) shows a negative anomaly that extends on both sides of the Alboran Sea. Although the area of thick continental crust located in the central part of the Rif is characterized by Bouguer anomalies reaching up to -150 mGal, the anomaly increases toward thinner crustal areas located at the foreland basins and the Alboran Basin, locally reaching up to $+50$ mGal near the outcrops of peridotite bodies. This regional increase toward the north reflects the transition from the thick continental crust of the Rif and the thin crust of the Alboran Sea. Bellot [1985] developed a detailed gravity study of the Beni Bousera peridotites, indicating that they are elongated near the coastline and extend northward up to the anomalous mantle of the Alboran Sea.

[16] A detailed aeromagnetic survey in northern Morocco was carried out in 1969–1970 by Compagnie Générale de la Géophysique (CGG) (unpublished reports of the Direction des Mines et de la Géologie du Maroc compiled by GETECH in the African Magnetic Mapping Project, 1989). The outstanding result was a narrow NW–SE elongated positive anomaly in the Rif Cordillera, bounded at the SE by the Jebha fault. This anomaly probably corresponds to the Beni Bousera peridotites outcropping in the Internal Zones (Figure 1).

4. Magnetotelluric Profile

4.1. Data Acquisition

[17] Eighteen magnetotelluric soundings were carried out in 2008 out for the first time along a 110 km NE-SW profile across the Rif Cordillera (Figure 1). The profile extends from Oued Laou, located in the Internal Zones and close to the Alboran coast, to the town of Mechra-Ben-Ksiri in the Gharb foreland basin. The profile is nearly orthogonal to the main regional geological

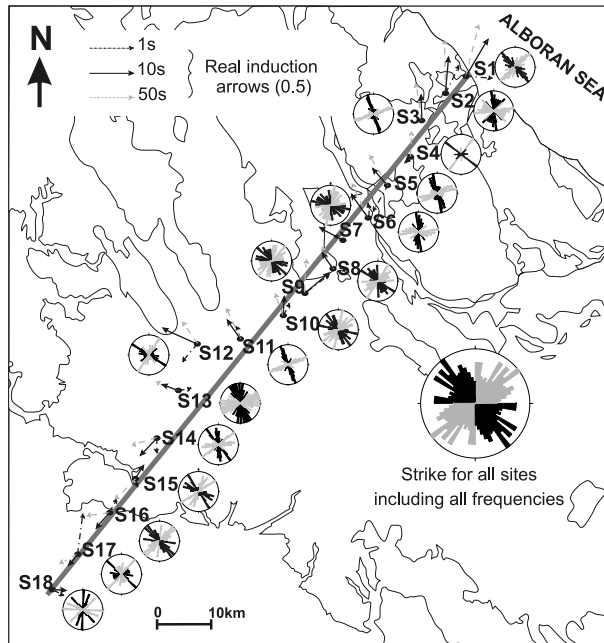


Figure 2. Real induction arrows at 1 s, 10 s, and 50 s (Parkinson's convention, pointing to conductors) for the 18 MT sites, and rose diagrams (Bahr's method) for every sounding including all frequencies on a contour geological sketch of the studied area and a common rose diagram for all the sites and all the frequencies.

structures, extending from the Internal Zones, and crossing the External Zones to the Gharb foreland basin. Magnetotelluric data were collected with Metronix ADU-07 equipment, covering a frequency band from 0.001 s to 1000 s. The registration time at each site was about 3 days. Impedance tensor components and the geomagnetic transfer functions were obtained through standard robust processing [Egbert and Booker, 1986]. Data quality was good for most of the stations, with local exceptions for some higher frequencies due to cultural noise.

4.2. Induction Arrows

[18] Induction arrows allow for a qualitative recognition of lateral conductivity contrasts. They point toward regions of highest conductivity and increase their magnitudes as the gradient of resistivity Parkinson convention [Parkinson, 1959].

[19] Figure 2 shows the real induction arrows at three different periods. The shortest period is related to the shallow structure whereas the longest period represents the deep structure. In general they have a moderate magnitude. At 1 s the vectors are heterogeneous, indicating a shallow heterogeneous resistivity. Vectors at 10 s and 50 s have similar

trends, pointing northeastward in the NE part of the profile, rotating to northwestward in the central part, and finally southwestward in the SW end.

4.3. Dimensionality Analysis

[20] The dimensionality analysis of the profile was undertaken using the Bahr method [Bahr, 1988]. Based on the rotational invariant and distortion parameters, it provides stable results even with noisy data.

[21] The dimensionality estimations have different degrees of distortion for each frequency band, and therefore a single sounding may present variable dimensionality at depth. The dimensionality analysis of all the sites and for all frequencies (Figure 3) suggests a generally two-dimensional structure at depth with some 3D influence at some sites.

[22] The estimated strike is shown in Figure 2 in rose diagrams for each site. The regional NW-SE elongated structure of the Rif is generally parallel to one maximum of the diagrams, suggesting the same dominant structure. However, induction arrows mainly in the central part of the profile indicate structures that are not perpendicular to the profile and therefore deviate from the 2D hypothesis. Thus, we proceeded as follows: First, a 2D inversion was performed, and then, the 2D inverse model was tested by simple 3D inversion. The extended 2D model along the strike was used as the initial model for the inversion. In line with Figure 2 and given the regional NW-SE elongated structure of the Rif, a preferential direction of N145°E was considered. This trend may be roughly regarded as the geoelectrical strike direction.

4.4. 2D Inversion

[23] In accordance with the dimensionality analyses, we preceded with 2D joint inversion [Rodi and Mackie, 2001] of the rotated (to -35°) apparent resistivities and phases and the projected geomagnetic transfer functions. TM and TE modes, corresponding to electric current flow perpendicular and parallel to the strike direction, respectively, were identified. The bathymetry of the Alboran sea was fixed in the inversion with a resistivity of 0.3 ohm.m. The final resistivity model (Figure 4) was obtained with a RMS of 2.4 using an error floor of 10% for apparent resistivities, 5% for phases and 0.1 for the tipper. The regularization parameter was $\tau = 3$, which was obtained by optimizing the trade-off between smoothing the model and lowering the

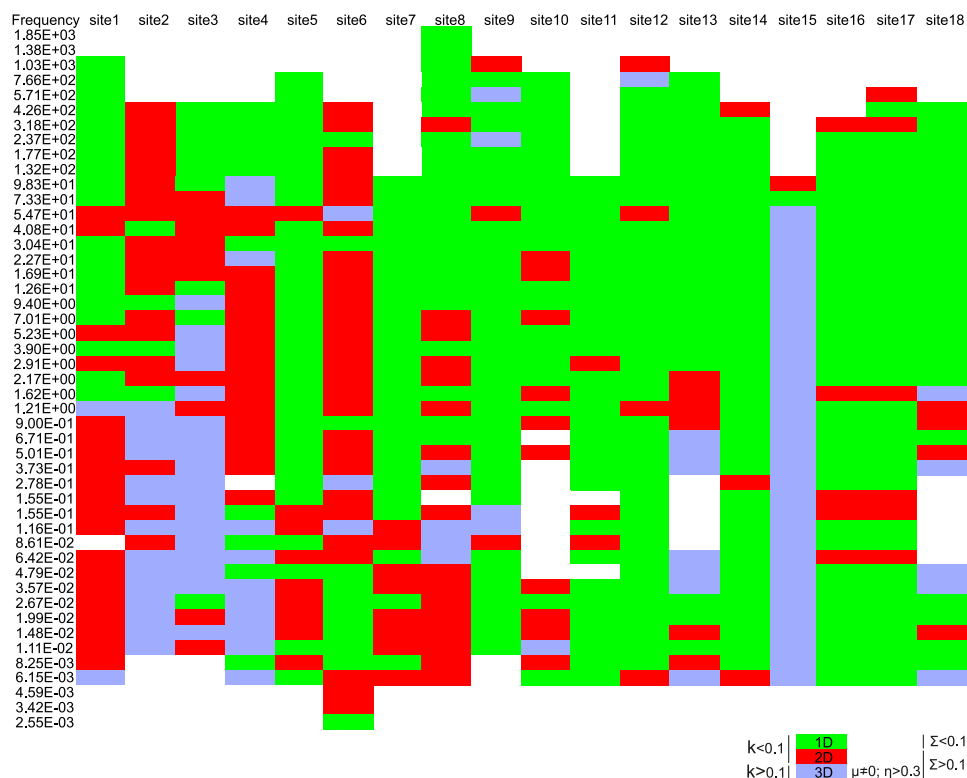


Figure 3. Dimensionality analysis of the MT data (Bahr's method) for all soundings and for all frequencies. k , Σ , μ , η are parameters proposed by *Bahr* [1988].

RMS misfit (L-curve, Figure 5). Figure 6 shows the responses of the model.

4.5. 2D Resistivity Model

[24] The electrical resistivity model along the upper crust (Figure 4) reveals a continuous conductive layer that in the SW (C1), reaches from the surface to a depth of 5 km (between site 18 and site 14) and thickens to the northeast. At the NE end of the

model, a resistive body (R3) extends from 4 km to 8 km beneath site 1, and is surrounded by conductive zones (C2) and the Alboran sea (C3).

[25] The middle and lower crust are dominated by high resistivities along the profile (R1, R2, R3), with the exception of the conductive zone beneath sites 9 and 10 (C4). Different sensitivity tests were carried out, changing the resistivities of the main features of the model; the result was always a large

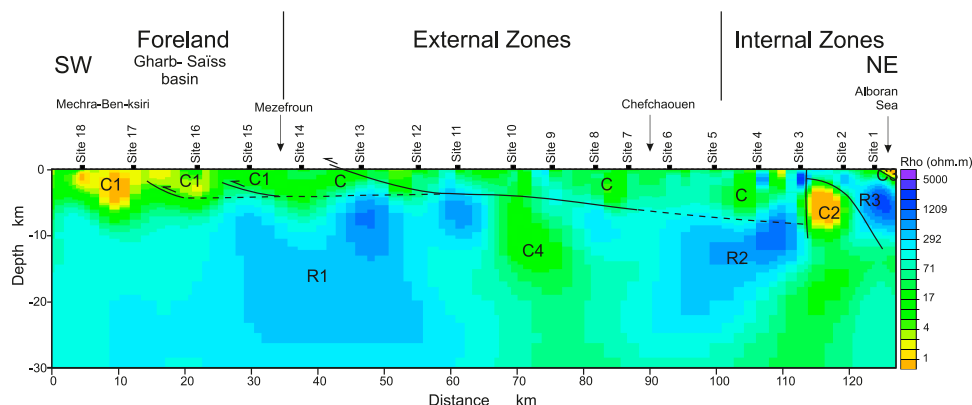


Figure 4. Magnetotelluric 2D model across the studied area. The conductive bodies are noted as C and the resistive bodies as R.

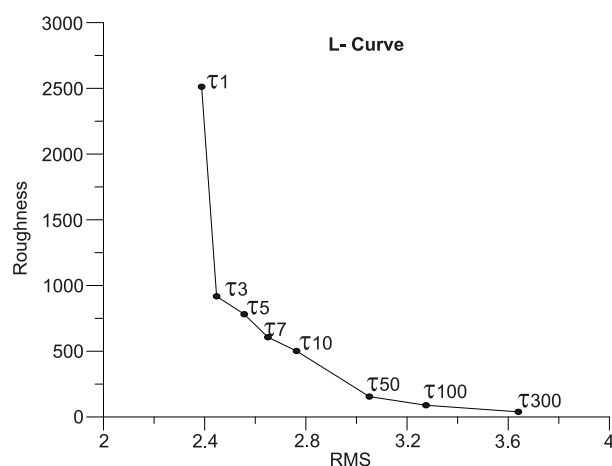


Figure 5. L curve, trade-off between model roughness and root mean square. $\tau = 3$ was chosen.

data misfit, with resolution decreasing only in the deepest parts of the model (>25 km).

5. 3D Inversion

[26] A 3D inversion of the impedance tensor was carried out using the WSINV3DMT code [Siripunvaraporn *et al.*, 2005]. The aim was to test the reliability of the 2D approach and search for possible structures along the strike. A selection of 8 sites along the profile was used as input data with 7 periods at each site (from 0.1 to 162 s). The input impedance data were not rotated. The mesh consisted of 45 cells in both x and y horizontal directions and 35 cells in the vertical z direction. Default values ($\tau = 5$ and $\delta = 0.1$) were used for the two parameters of the decorrelation scale controlling the model roughness [Siripunvaraporn *et al.*, 2005]. The starting model was built using the conductivity distribution from the 2D inversion model extended along the strike direction. The average cell size is 3×3 km in the horizontal plane (x, y directions). In the vertical z direction, the cell size increases from 100 m on average for the first layers to 2 km at 10 km depth and so on to more than 100 km where the cell size reaches 20 km. The inversion was prepared for a maximum of 10 iterations and a normalized minimum RMS of 2.73 was obtained in iteration 6. Figure 7 shows the data input and model responses for each of the sites used in the 3D inversion. Apparent resistivities and phases are preferred for the figure instead of the impedances that are used in the inversion. Note that diagonal phases are plotted in the quadrant where they appeared. The change of quadrant for different periods is due to the instability (small magnitudes)

of the impedance diagonal components. Figure 8 shows the final 3D model in terms of 3 vertical cross sections: the central panel corresponds to the central part of the 3D model, just below the sites, the upper panel is 30 km to the west, and the lower panel is 30 km to the east. Figure 9 shows a plan view at 15 km depth. As we can see, the central section reproduces quite well the 2D inverse model in Figure 4. To the SW, the shallow conductors correspond to sequence C1 in Figure 4; whereas to the NE, beneath site 2, the 3 conductive columns at shallow crustal depth correlate with conductor C2 in Figure 4. The middle-upper crust is highly resistive along the model interrupted by the conductor beneath sites 9 and 10, in agreement with the 2D model in Figure 4. The cross sections at both sides of the profile (Figure 8) show slight variations of the resistivity distribution compared with the central section. However, these variations suffice to explain the behavior of some induction arrows which deviate to the assumed 2D strike direction. Unfortunately, the 3D inversion code used does not include the inversion of the tipper. Forward modeling of the 3D inverse model was carried out by using the algorithm of Mackie *et al.* [1993] [Mackie and Booker, 1999]. Figure 9 shows the real induction arrows at 10 s and 100 s. Note that some of the induction arrows now deviate from the direction of the profile. No large conductor to the west of the profile was needed to explain this behavior. Comparison of the resistivity sections at both sides of the central section (Figure 8) shows that the significant difference is that toward NW (Figure 8, top) there is a slight increase in the conductive area together with a generalized but also slight decrease in the resistive zone in the middle-upper crust. This can also be seen in plan view at 15 km depth in Figure 9.

[27] Thus, the main conductive features of the 2D inverse model remain in the 3D inversion, reinforcing the 2D model (Figure 4). A 3D inversion of only 1 MT profile may yield a large range of conductive structures at a distance from the current profile, and only new data to the west could confirm these slight increases in conductivity.

6. Discussion

[28] In recent years, different geophysical studies have attempted to constrain the crustal and mantle structure of the Betic-Rif cordillera, located at the westernmost end of the Mediterranean alpine belt. Recent geological and geophysical surveys in the Alboran Sea and Rif cordillera are sparse, however,

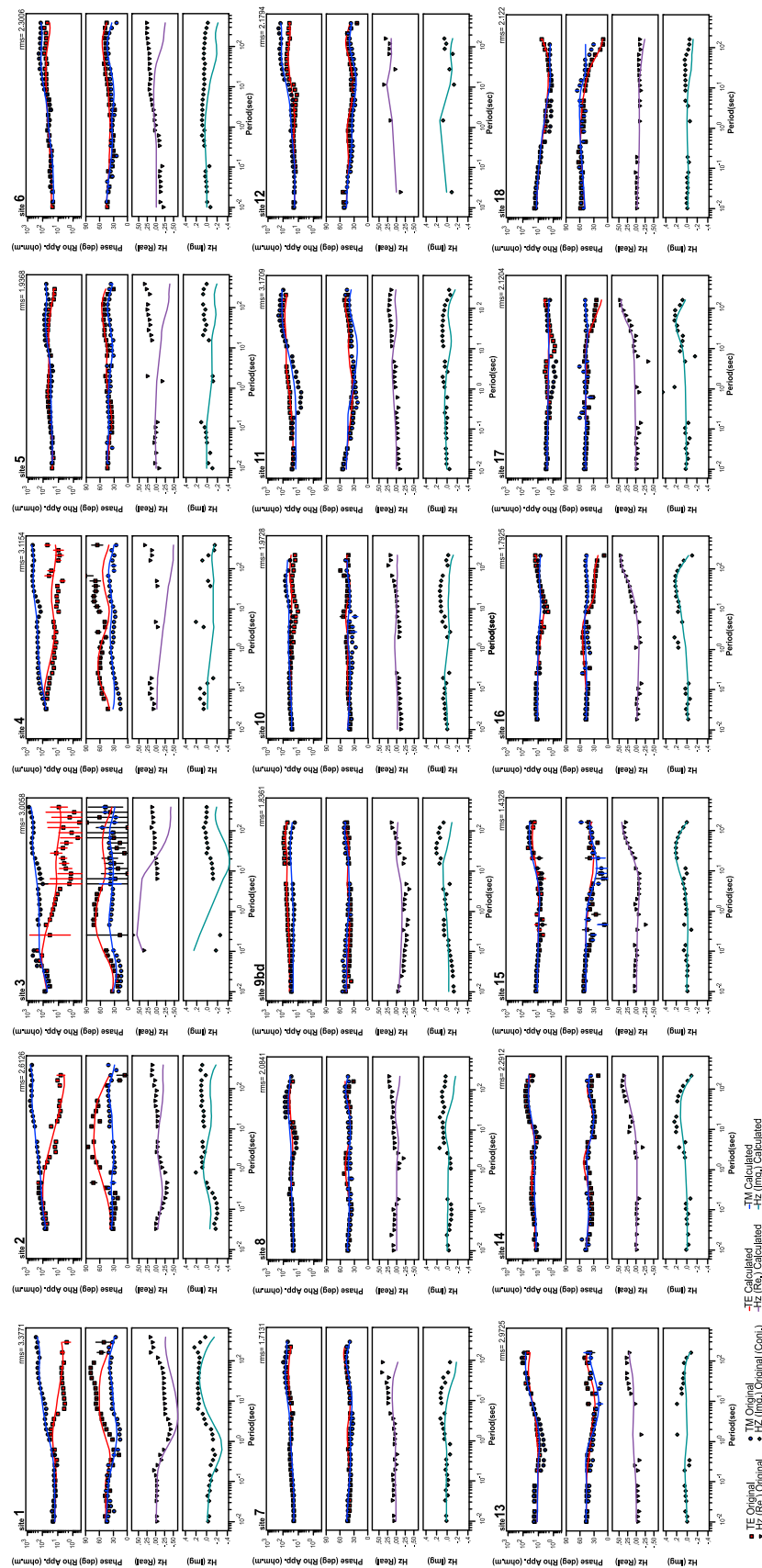


Figure 6. Data and model responses of the 2D model of Figure 4. Apparent resistivities and phases are rotated to -35° and the geomagnetic transfer functions projected.

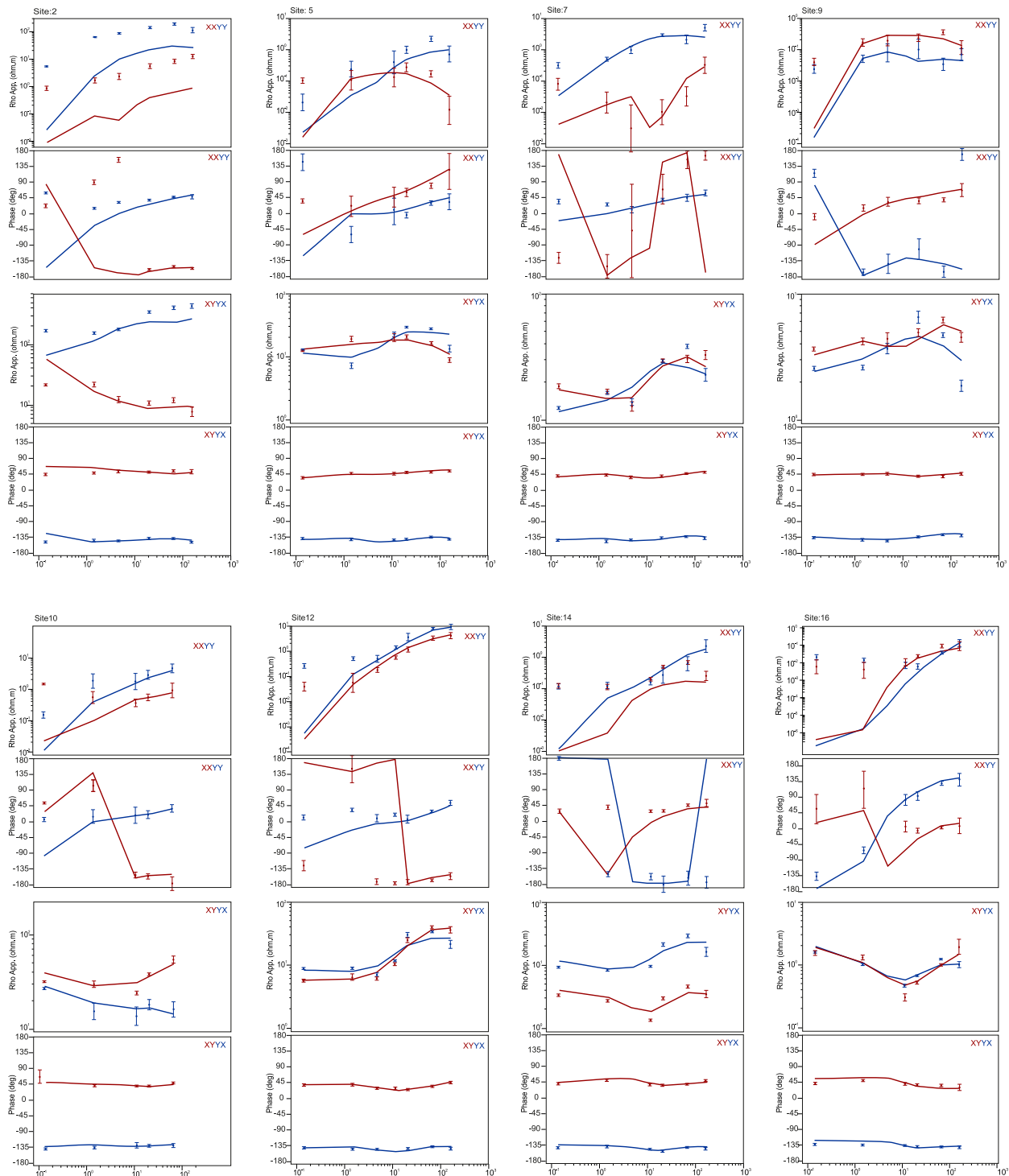


Figure 7. Unrotated data and model responses of the 3D inverse model.

unlike the Betic cordillera [Galindo-Zaldívar *et al.*, 1997; Pous *et al.*, 1999; Serrano *et al.*, 2003; Martí *et al.*, 2004], mainly because of the harsh topography and scarce roads. The lack of geophysical and geological data in the region impedes determination

of the deep structures that would support the proposal of new geological evolution models. In this context, crustal models are inferred from very indirect data such as surface motions [Pérouse *et al.*, 2010]. The two-dimensional resistivity model

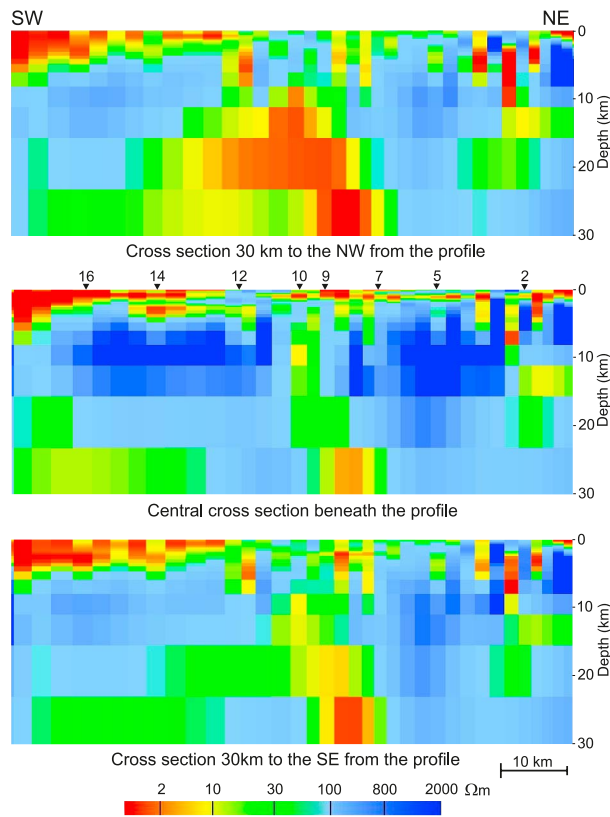


Figure 8. Vertical sections of the 3D model. (top) 30 km to the west of the profile. (middle) Beneath the MT profile in the central part of the 3D model. (bottom) 30 km to the east of the profile.

of the MT data (Figure 4) in agreement with the 3D inversion (Figure 8) shows a good correlation with other geophysical data [Van den Bosch, 1971, 1981; Hatzfeld and Ben Sari, 1977; Bellot, 1985] confirming that the crustal structure is formed by the overprinting of alpine Rif tectonic units on a deep basement (Figure 10), probably corresponding to the northward continuity of the variscan Moroccan Meseta. These two main domains are separated by a sharp detachment level that becomes shallow toward the SW and reaches approximately 10 km depth at the NE end of the profile. The model suggests a heterogeneous upper crust (Figures 4 and 10). The Internal Zones are formed by an outstanding low-resistivity body (C2) whose top lies at 4 km depth, probably corresponding to the nearby outcropping Beni Bousera peridotites (Figure 1), and a highly resistive body (R3) that is interpreted as metamorphic rocks (gneisses). Both C2 and R3 are considered as the NW continuity in depth of the peridotites and gneisses, respectively, which may correspond to elongated discontinuous bodies surrounding the western Gibraltar Arc. They are in agreement with gravity studies [Bellot, 1985] that support the extension of peridotite bodies parallel to the Alboran coast, although the size obtained with MT data is lesser than in gravity studies. To the north, the C3 body corresponds to conductive Alboran Seawater. Southward, the External Zones and the foreland Gharb basin are characterized by low resistivity values (C1, C),

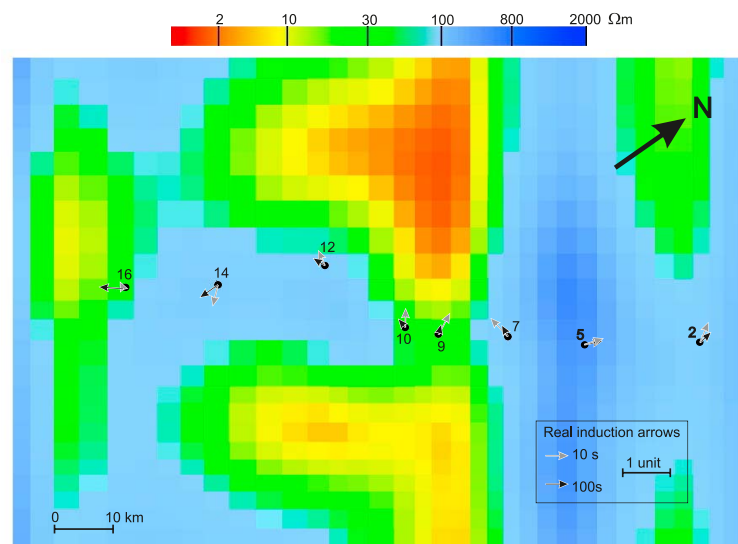


Figure 9. Plan view of the 3D model at 15 km depth. Dots are the MT sites used in the 3D inversion and real induction arrows at 10 and 100 s (Parkinson convention) corresponding to the 3D model are shown.

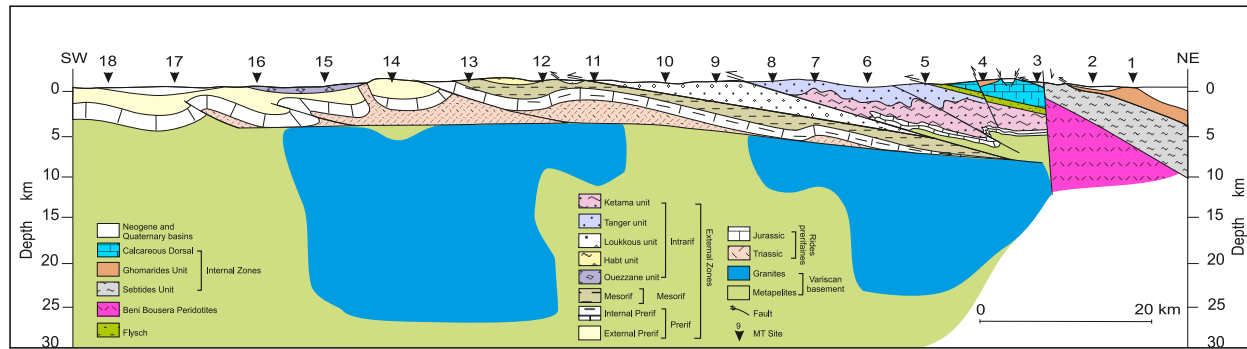


Figure 10. Deep section across the western Rif cordillera combining geological and magnetotelluric data.

corresponding to sedimentary rocks. Their bottom is interpreted as a thrust whose frontal part crops out southwest of Mezefroun (Figures 1 and 10). Moreover, the variable thickness of the highly conductive bodies of the External Zone front and the Gharb basin suggests the presence of basement highs that may be related to blind frontal thrusts (Figures 4 and 10).

[29] The most relevant feature in depth corresponds to a large high-resistivity body (R1 and R2), located below the frontal part of the Rif and between the Internal and External Zones (Figures 4 and 10). Situated in the middle and upper crust, and separated by a more conductive zone (C4), these resistive anomalies are located at a depth roughly below 5 km, having a very wide cross-section and extending over 25–40 km. The bodies feature an irregular upper boundary and extends in depth, although the base is not well constrained. The presence of exotic granitic and gneissic blocks at surface in some tectonic units of the frontal part of the Rif Cordillera [Ben Yaich, 1991] and also in boreholes [Faugères, 1978], along with their resistive character, would suggest that the large body (R1) corresponds to a granitic or gneissic basement surrounded by metapelitic rocks. The resistive body (R2) also agrees with the structure of the Moroccan Meseta, where kilometer-sized resistive late variscan granite bodies are emplaced in metapelitic host rocks [Michard et al., 2008].

[30] Conductors in the crust are usually detected in MT studies. The meaning of the conductors depends on the geodynamic conditions of each particular case. In the Rif, an active alpine chain, they are probably related to fluids or the presence of graphite-bearing schist. The point is that conductor C4 beneath sites 9 and 10 is too diffuse from the upper crust to the middle-lower crust. If this conductor appeared more elongated, then fluids along a fault zone would be a plausible explanation, but the

conductor beneath site 9 and 10 does not have this usual shape. Another possibility is the presence of a basement including graphite-bearing rocks, as occurs in the SW Iberia [Monteiro-Santos et al., 2002].

[31] The presence of shallow granitic or gneissic bodies below the External Zones and near the major detachment faults (Figure 10) suggests a possible model for emplacement at surface along the External Zones of exotic gneissic and metamorphic blocks. Detachment faults may have cut the top of the variscan basement and mixed the blocks with the low density Triassic cover formed by clays and evaporites that constitutes the base of the alpine tectonic units. Therefore, shearing during frontal accretion and diapiric processes associated with the Triassic rocks may have allowed emplacement up to the surface of the basement metamorphic rocks (Figure 10, between sites 14 and 15). In the resistivity model (Figure 4), the small conductive body could represent the ascending diapiric structure. Recent GPS observations suggest active southwestward motion of the Rif Cordillera with respect to the Moroccan Meseta, in a trend parallel to the obtained MT profile [Pérouse et al., 2010]. Although this research associated active motion to the presence of a NE-dipping subduction zone that affects the Rif, our geophysical data do not support such an interpretation, as we do not envisage continuity in deep bodies toward the NE. Southwestward motions may be interpreted as evidence of the activity of the main detachment located below the alpine orogenic wedge [Chalouan et al., 2006; Pedrera et al., 2011], constrained from the magnetotelluric data presented here.

7. Conclusions

[32] New magnetotelluric data provide an image of crustal resistivity along a NE-SW transect of the Rif

Cordillera and its foreland basin, helping to complete the surface geological observations. These data allow us to determine the major deep structures in this area, despite scarce previous geophysical data, and to constrain the relationship between shallow and deep crustal structures.

[33] The resistivity 2D model (Figure 4) confirmed by the 3D inversion (Figure 8) shows overprinting of the Rif alpine tectonic units on the Moroccan Meseta basement, separated by a major active northeastward dipping crustal detachment with top-to-the-SW kinematics. The Gharb basin features irregular sedimentary infill, most likely related to the presence of blind thrusts associated with frontal Rif deformations. The Internal Rif has greater resistivity heterogeneity than the External Rif, where moderately conductive bodies prevail. One outstanding conductive body in the shallow upper crust near the Alboran Sea is interpreted as the northwestward continuity in depth of the Beni Bousera peridotites. Overlying it is a nearby resistive body corresponding to micaschists and gneisses belonging to the Sebide Complex. The Rif basement is attributed to the variscan Moroccan Meseta, characterized by large resistive bodies, probably corresponding to granites and gneisses, emplaced in a metapelitic host rock.

[34] The exotic metapelitic and gneissic rocks observed in the frontal part of the Rif Cordillera, whose lithology is different from the rocks of the internal Rif units, probably came from the underlying variscan basement. The activity of the basal detachment may have contributed to fracturing the top of the basement, which was mixed with the Triassic evaporites and clays and finally emplaced in the surface.

[35] The southern part of the Gibraltar Arc is a key region for discussion of the geodynamical models proposed in the context of Alboran Sea evolution. The new data on the top-to-the-SW Rif orogenic wedge would support the present-day models based on subduction developing crustal thrust structures, rather than models based on delamination.

Acknowledgments

[36] The constructive comments of G. Muñoz, D. Stanica and K. Bahr have improved this manuscript. Projects CSD2006-00041, CGL2008-03474-E/BTE, CGL2010-21048, P09-RNM-5388 and RNM148 are acknowledged.

References

- Azdimousa, A., J. Bourgeois, G. Poupeau, and R. Montigny (1998), Histoire thermique du massif de Ketama (Maroc): Sa place en Afrique du Nord et dans les Cordillères bétiques, *C. R. Acad. Sci., Ser. IIa*, 326, 847–853.
- Bahr, K. (1988), Interpretation of the magnetotelluric impedance tensor: Regional induction and local telluric distortion, *J. Geophys.*, 62, 119–127.
- Bellet, A. (1985), Etude Gravimétrique du Rif Paléozoïque: La Forme du Massif des Beni Bousera, Ph.D. thesis, Univ. Montpellier 2, Montpellier, France.
- Benmakhlouf, M., and A. Chalouan (1995), Evolution Néogène du bassin de Tétouan-Martil, Rif septentrional, Maroc, *Geogaceta*, 17, 98–100.
- Ben Yaich, A. (1991), Evolution tectono-sédimentaire du Rif externe centre-occidental (régions de M'Sila et Ouezzane, Maroc): La marge africaine du Jurassique au Crétacé; les bassins néogènes d'avant-fosse, Ph.D. thesis, Univ. de Pau et des Pays de l'Adour, Pau, France.
- Bokelmann, G., and E. Maufroy (2007), Mantle structure under Gibraltar constrained by dispersion of bodywaves, *Geophys. Res. Lett.*, 34, L22305, doi:10.1029/2007GL030964.
- Bouybaouene, M. L., B. Goffé, and A. Michard (1998), High-pressure granulites on top of the Beni Bousera peridotites, Rif Belt, Morocco: A record of an ancient thickened crust in the Alboran domain, *Bull. Soc. Geol. Fr.*, 169, 153–162.
- Brun, J. P., and C. Faccenna (2008), Exhumation of high-pressure rocks driven by slab rollback, *Earth Planet. Sci. Lett.*, 272, 1–7, doi:10.1016/j.epsl.2008.02.038.
- Calvert, A., E. Sandvol, D. Seber, M. Barazangi, S. Roecker, T. Mourabit, F. Vidal, G. Alguacil, and N. Jabour (2000), Geodynamic evolution of the lithosphere and upper mantle beneath the Alboran region of the western Mediterranean: Constraints from travel time tomography, *J. Geophys. Res.*, 105(B5), 10,871–10,898.
- Chalouan, A., and A. Michard (1990), The Ghomarides nappes, Rif coastal Range, Morocco: A Variscan chip in the Alpine belt, *Tectonics*, 9, 1565–1583, doi:10.1029/TC009i006p01565.
- Chalouan, A., A. Ouazani-Touhami, L. Mouhir, R. Saji, and M. Benmakhlouf (1995), Les failles normales à faible pendage du Rif interne (Maroc) et leur effet sur l'aminicissement crustal du domaine d'Alboran, *Geogaceta*, 17, 107–109.
- Chalouan, A., et al. (2006), Tectonic wedge escape in the southwestern front of the Rif Cordillera (Morocco), in *Tectonics of the Western Mediterranean and North Africa*, edited by G. Moratti and A. Chalouan, *Geol. Soc. Spec. Publ.*, 262, 183–280.
- Cirac, P. (1987), Le Bassin sudrifain au Néogène supérieur. Évolution de la dynamique sédimentaire et de la paléogéographie au cours d'une phase de comblement, *Mem. Inst. Geol. Bassin Aquitaine*, 21, 1–287.
- Egbert, G. D., and J. R. Booker (1986), Robust estimation of geomagnetic transfer functions, *Geophys. J. R. Astron. Soc.*, 87, 173–194.
- El Kadiri, K., A. Linares, and F. Oloriz (1992), La Dorsale calcaire rifaine (Maroc septentrional): Evolution stratigraphique et géodynamique durant le Jurassique-Crétacé, *Notes Mem. Serv. Geol.*, 336, 217–265.
- El Mirihi, A. (2005), Structure et cinématique de la mise en place des nappes des flyschs maurétaniens (Rif externe nord oriental): Elaboration d'un modèle, Ph.D. thesis, Univ. de Tetuan, Tetuan, Morocco.

- Fadil, A., P. Vernant, S. McClusky, R. Reilinger, F. Gomez, D. Ben Sari, T. Mourabit, K. Feigl, and M. Barazangi (2006), Active tectonics of the western Mediterranean: Geodetic evidence for rollback of a delaminated subcontinental lithospheric slab beneath the Rif Mountains, Morocco, *Geology*, **34**, 529–532, doi:10.1130/G22291.1.
- Faugères, J. C. (1978), Les Rides sud-rifaines: évolution sédimentaire et structural d'un bassin atlantico mésogéen de la marge africaine, Ph.D. thesis, Univ. de Bordeaux I, Talence, France.
- Flinch, J. F. (1993), Tectonic evolution of the Gibraltar Arc. Ph.D. thesis, Rice Univ., Houston, Tex.
- Frizon de Lamotte, D. (1985), La structure du Rif oriental (Maroc). Rôle de la tectonique longitudinale et importance des fluides, *Mem. Sci. Univ. Curie, Paris*, **85-03**, 1–436.
- Fullea, J., M. Fernández, H. Zeyen, and J. Vergés (2007), A rapid method to map the crustal and lithospheric thickness using elevation, geoid anomaly and thermal analysis. Application to the Gibraltar Arc System, Atlas Mountains and adjacent zones, *Tectonophysics*, **430**, 97–117, doi:10.1016/j.tecto.2006.11.003.
- Galindo-Zaldívar, J., A. Jabaloy, F. González Lodeiro, and F. Aldaya (1997), Crustal structure of the central sector of the Betic Cordillera SE Spain, *Tectonics*, **16**, 18–37, doi:10.1029/96TC02359.
- Hatzfeld, D., and D. Ben Sari (1977), Grands profils sismiques dans la région de l'arc de Gibraltar, *Bull. Soc. Geol. Fr.*, **7**, 749–756.
- Kornprobst, J. (1974), Contribution à l'étude pétrographique et structurale de la Zone interne du Rif (Maroc septentrional), *Notes Mem. Serv. Geol.*, **251**, 1–256.
- Le Coz, J. (1964), Le Rharb, Fellahs et colons. Étude de géographie régionale, Ph.D. thesis, Univ. Rabat, Rabat.
- Lespinasse, P. (1975), Géologie des zones externes et des flyschs entre Chaouen et Zoumi (Centre de la Chaîne rifaine, Maroc), Ph.D. thesis, Univ. Pierre et Marie Curie, Paris.
- Litto, W., E. Jaaidi, M. Dakki, and F. Medina (2001), Etude sismo-structurale de la marge nord du bassin du Gharb (avant-pays rifain, Maroc): Mise en évidence d'une distension d'âge miocène supérieur, *Eclogae Geol. Helv.*, **94**, 63–73.
- Loneragan, L., and N. White (1997), Origin of the Betic-Rif mountain belt, *Tectonics*, **16**, 504–522, doi:10.1029/96TC03937.
- Maaté, A. (1996), Estratigrafia y evolucion paleogeografica alpina del dominio gomaride (Rif interno, Marruecos), Ph.D. thesis, Univ. Granada, Granada, Spain.
- Mackie, R., and J. R. Booker (1999), *Documentation for mtd3fwd and d3-to-mt*, GSY-USA, Inc., San Francisco, Calif.
- Mackie, R. L., T. R. Madden, and P. E. Wannamaker (1993), Three-dimensional magnetotelluric modeling using difference equations—Theory and comparison to integral equation solutions, *Geophysics*, **58**, 215–226, doi:10.1190/1.1443407.
- Martí, A., P. Queralt, and E. Roca (2004), Geoelectric dimensionality in complex geologic areas: Application to the Spanish Betic Chain, *Geophys. J. Int.*, **157**, 961–974, doi:10.1111/j.1365-246X.2004.02273.x.
- Michard, A., A. Chalouan, R. Montigny, and M. Ouazzani-Touhami (1983), Les nappes cristallophylliennes du Rif (Sebtides, Maroc), temoins d'un edifice alpin de type pennique incluant le manteau superieur, *C. R. Acad. Sci., Ser. II*, **296**, 1337–1340.
- Michard, A., C. Hoepffner, A. Soulaïmani, and L. Baidder (2008), The variscan Belt, in *The Geology of Morocco, Lect. Notes Earth Sci.*, vol. 116, edited by A. Michard et al., pp. 65–133, Springer, New York.
- Monteiro Santos, F. A., A. Mateus, E. P. Almeida, J. Pous, and L. A. Mendes-Victor (2002), Are some of the deep crustal features found in SW Iberia caused by graphite?, *Earth Planet. Sci. Lett.*, **201**, 353–367, doi:10.1016/S0012-821X(02)00721-5.
- Morley, C. K. (1993), Discussion of origins of hinterland basins to the RIF-Betic Cordillera and Carpathians, *Tectonophysics*, **226**, 359–376, doi:10.1016/0040-1951(93)90127-6.
- Nold, M., J. Uttinger, and W. Wildi (1981), Géologie de la Dorsale calcaire entre Tétouan et Assifane (Rif interne, Maroc), *Notes Mem. Serv. Geol.*, **300**, 1–233.
- Parkinson, W. (1959), Directions of rapid geomagnetic fluctuations, *Geophys. J. R. Astron.*, **2**, 1–14.
- Pedrerá, A., et al. (2011), Is there an active subduction beneath the Gibraltar orogenic arc? Constraints from Pliocene to present-day stress field, *J. Geodyn.*, **52**, 83–96, doi:10.1016/j.jog.2010.12.003.
- Pérouse, P., P. Vernant, J. Chéry, R. Reilinger, and S. McClusky (2010), Active surface deformation and sub-lithospheric processes in the western Mediterranean constrained by numerical models, *Geology*, **38**, 823–826, doi:10.1130/G30963.1.
- Platt, J. P., and R. L. M. Vissers (1989), Extensional collapse of thickened continental lithosphere, a working hypothesis for the Alboran Sea and Gibraltar Arc, *Geology*, **17**, 540–543, doi:10.1130/0091-7613(1989)017<0540:ECOTCL>2.3.CO;2.
- Pous, J., P. Queralt, J. Ledo, and E. Roca (1999), A high electrical conductive zone at lower crustal depth beneath the Betic Chain Spain, *Earth Planet. Sci. Lett.*, **167**, 35–45, doi:10.1016/S0012-821X(99)00011-4.
- Rodi, W. L., and R. L. Mackie (2001), Nonlinear conjugate gradients algorithm for 2-D magnetotelluric inversion, *Geophysics*, **66**, 174–187, doi:10.1190/1.1444893.
- Royden, L. H. (1993), Evolution of retreating subduction boundaries formed during continental collision, *Tectonics*, **12**, 629–638, doi:10.1029/92TC02641.
- Saddiqi, O. (1995), Exhumation des roches profondes, péridotites et roches métamorphiques HP-BT dans deux transects de la chaîne alpine: Arc de Gibraltar et Montagnes d'Oman, Ph.D. thesis, Univ. Hassan II, Casablanca, Morocco.
- Saji, R., and A. Chalouan (1995), Le bassin pliocène intramontagneux du Tirinense et son mode d'ouverture (Rif interne, Maroc), *Geogaceta*, **17**, 110–112.
- Seber, D., M. Barazangi, B. A. Tadili, M. Ramdani, A. Ibenbrahim, and D. Ben Sari (1996), Three dimensional upper mantle structure beneath intraplate Atlas and interplate Rif mountains of Morocco, *J. Geophys. Res.*, **101**, 3125–3138, doi:10.1029/95JB03112.
- Serrano, I., D. Zhao, J. Morales, and F. Torcal (2003), Seismic tomography from local crustal earthquakes beneath Eastern Rif Mountains of Morocco, *Tectonophysics*, **367**, 187–201, doi:10.1016/S0040-1951(03)00100-8.
- Siripunvaraporn, W., G. Egbert, and Y. Lenbry (2005), Three-dimensional magnetotelluric inversion: Data-space method, *Phys. Earth Planet. Inter.*, **150**, 3–14, doi:10.1016/j.pepi.2004.08.023.
- Suter, G. (1980), Carte géologique du Rif, 1/500.000, *Map 245a*, Geol. Surv. of Morocco, Rabat.
- Van den Bosch, J. W. H. (1971), Carte gravimétrique du Maroc, scale 1:500.000, *Map 234a*, Geol. Surv. of Morocco, Rabat.

- Van den Bosch, J. W. H. (1981), Mémoire explicatif de la carte gravimétrique du Maroc (province du Nord) au 1/500 000, *Notes Mem. Serv. Geol.*, 234b, 1–219.
- Vernant, P., A. Fadil, T. Mourabit, D. Ouazar, A. Koulali, J. M. Davila, J. Garate, S. McClusky, and R. E. Reilinger (2010), Geodetic constraints on active tectonics of the Western Mediterranean: Implications for the kinematics and dynamics of the Nubia-Eurasia plate boundary zone, *J. Geodyn.*, 49, 123–129, doi:10.1016/j.jog.2009.10.007.
- Weijermars, R., M. P. A. Jackson, and B. Vendeville (1993), Rheological and tectonic modelling of salt provinces, *Tectonophysics*, 217, 143–174, doi:10.1016/0040-1951(93)90208-2.
- Wildi, W. (1983), La chaîne tello-rifaine (Algérie, Maroc, Tunisie): Structure, stratigraphie et évolution du Trias au Miocène, *Rev. Geol. Dyn. Geogr. Phys.*, 24, 201–297.
- Zeyen, H., P. Ayarza, M. Fernández, and A. Rimi (2005), Lithospheric structure under the western African-European plate boundary: A transect across the Atlas Mountains and the Gulf of Cadiz, *Tectonics*, 24, TC2001, doi:10.1029/2004TC001639.
- Zizi, M. (1996), Triassic-Jurassic extension and Alpine inversion in Northern Morocco, in *Peri-Tethys Memoir 2: Structure and Prospects of Alpine Basins and Forelands*, edited by P. Ziegler and F. Horvath, *Mem. Mus. Natl. Hist. Nat.*, 170, 87–101.